An Extensive Program of Periodic Alternative Splicing Linked to Cell Cycle Progression

Authors:

Daniel Dominguez[1,2], Yi-Hsuan Tsai[1,3], Robert Weatheritt [4], Yang Wang[1,2],

Benjamin J. Blencowe [* 4], Zefeng Wang[* 1,5]

Affiliations:

[1] Department of Pharmacology, University of North Carolina at Chapel Hill, Chapel Hill, NC

[2] Lineberger Comprehensive Cancer Center, University of North Carolina at Chapel Hill, Chapel Hill, NC

[3] Program in Bioinformatics and Computational Biology, University of North Carolina at Chapel Hill, Chapel Hill, NC,

[4] Donnelly Centre and Department of Molecular Genetics, University of Toronto, Canada

[5] Key Lab of Computational Biology, CAS-MPG Partner Institute for Computational Biology, Chinese Academy of Science, Shanghai, China

*** Correspondence to: zefeng@med.unc.edu; b.blencowe@utoronto.ca**

Abstract

Progression through the mitotic cell cycle requires periodic regulation of gene function at the levels of transcription, translation, protein-protein interactions, post-translational modification and degradation. However, the role of alternative splicing (AS) in the temporal control of cell cycle is not well understood. By sequencing the human transcriptome through two continuous cell cycles, we identify ~1,300 genes with cell cycle-dependent AS changes. These genes are significantly enriched in functions linked to cell cycle control, yet they do not significantly overlap genes subject to periodic changes in steady-state transcript levels. Many of the periodically spliced genes are controlled by the SR protein kinase CLK1, whose level undergoes cell cycle-dependent fluctuations via an auto-inhibitory circuit. Disruption of CLK1 causes pleiotropic cell cycle defects and loss of proliferation, whereas CLK1 over-expression is associated with various cancers. These results thus reveal a large program of CLK1-regulated periodic AS intimately associated with cell cycle control.

Impact statement

We reveal extensive periodic regulation of alternative splicing during the cell cycle in genes linked to cell cycle functions, and involving an auto-inhibitory mechanism employing the SR protein kinase CLK1.

Introduction

Alternative splicing (AS) is a critical step of gene regulation that greatly expands proteomic diversity. Nearly all (>90%) human genes undergo AS and a substantial fraction of the resulting isoforms are thought to have distinct functions (Pan et al., 2008; Wang et al., 2008). AS is tightly controlled, and its mis-regulation is a common cause of human diseases (Wang and Cooper, 2007). Generally, AS is regulated by *cis*-acting splicing regulatory elements that recruit *trans*-acting splicing factors to promote or inhibit splicing (Matera and Wang, 2014; Wang and Burge, 2008). Alterations in splicing factor expression have been observed in many cancers and are thought to activate cancer-specific splicing programs that control cell cycle progression, cellular proliferation and migration (David and Manley, 2010; Oltean and Bates, 2014). Consistent with these findings, several splicing factors function as oncogenes or tumor suppressors (Karni et al., 2007; Wang et al., 2014), and cancer-specific splicing alterations often affect genes that function in cell cycle control (Tsai et al., 2015).

Progression through the mitotic cell cycle requires periodic regulation of gene function that is primarily achieved through coordination of protein levels with specific cell cycle stages (Harashima et al., 2013; Vermeulen et al., 2003). This temporal coordination enables timely control of molecular events that ensure accurate chromatin duplication and daughter cell segregation. Periodic gene function is conventionally thought to be achieved through stage-dependent gene transcription (Bertoli et al., 2013), translation (Grabek et al., 2015), protein-protein interactions (Satyanarayana and Kaldis, 2009), post-translational protein modifications, and ubiquitin-dependent protein degradation (Mocciaro and Rape, 2012). Although AS is one of the most widespread mechanisms involved in gene regulation, the relationship between the global coordination of AS and the cell cycle has not been investigated.

Major families of splicing factors include the Serine-Arginine rich proteins (SR) proteins and the heterogeneous nuclear ribonucleoproteins (hnRNPs), whose levels and activities vary across cell types. SR proteins generally contain one or two RNA recognition motifs (RRMs) and a domain rich in alternating Arg and Ser residues (RS domain). Generally, RRM domains confer RNA binding specificity while the RS domain mediates protein-protein and protein-RNA interactions to affect splicing (Long and Caceres, 2009; Zhou and Fu, 2013). Post-translational modifications of SR proteins, most notably phosphorylation, modulate their splicing regulatory capacity by altering protein localization, stability or activity (Gui et al., 1994; Lai et al., 2003; Prasad et al., 1999; Shin and Manley, 2002). Dynamic changes in SR protein phosphorylation have been detected after DNA damage (Edmond et al., 2011; Leva et al., 2012) and during the cell cycle (Gui et al., 1994; Shin and Manley, 2002), suggesting that regulation of AS may have important roles in cell cycle control. However, the functional consequences of SR protein (de)phosphorylation during the cell cycle are largely unclear.

Through a global-scale analysis of the human transcriptome at single-nucleotide resolution through two continuous cell cycles, we have identified widespread periodic changes in AS that are coordinated with specific stages of the cell cycle. These periodic AS events belong to a set of genes that is largely separate from the set of genes periodically regulated during the cell cycle at the transcript level, yet the AS regulated set is significantly enriched in cell cycle-associated functions. We further demonstrate that a significant fraction of the periodic AS events is regulated by the SR protein kinase, CLK1, and that CLK itself is also subject to cell cycle-dependent regulation. Moreover, inhibition or depletion of CLK1 causes pleiotropic defects in mitosis that lead to cell death or G1/S arrest, suggesting that the temporal regulation of splicing by CLK1 is critical for cell cycle progression. The discovery of periodic AS thus reveals a

widespread yet previously underappreciated mechanism for the regulation of gene function during the cell cycle.

Results

Alternative splicing is coordinated with different cell cycle phases

To systematically investigate the regulation of AS during the cell cycle, we performed an RNA-Seq analysis of synchronously dividing cells using a total of 2.3 billion reads generated across all stages (G1, S, G2 and M) of two complete rounds of the cell cycle (Figure 1-figure supplement 1A). To maximize the detection of regulated AS events, we used the complementary analysis pipelines, MISO and VAST-TOOLS (Katz et al., 2010; Irimia et al., 2014). These pipelines have different detection specificities and employ partially overlapping reference sets of annotated AS events, and therefore afford a more comprehensive analysis when employed together. Both pipelines were used to determine PSI (the percent of transcript with an exon spliced in) and PIR (the percent of transcripts with an intron retained). Alternative exons detected by both pipelines had highly correlated PSI values (Figure 1-figure supplement 1G; see below). Consistent with previous results (Bar-Joseph et al., 2008; Whitfield et al., 2002), transcripts from approximately 14.2% (1,182) of expressed genes displayed periodic differences in steady-state levels between two or more cell cycle stages (see below). Remarkably, 15.6% (1,293) of expressed genes also contained 1,747 periodically-regulated AS events, among a total of ~40,000 detected splicing events (FDR < 2.5%; Figure 1A and Figure 1-figure supplement 1B, 1C, 1D).

Importantly, as has been observed previously for AS regulatory networks (Pan et al., 2004), the majority of genes with periodic AS events did not overlap those with periodic steady-

state changes in mRNA expression. This indicates that genes with periodic changes in AS and transcript levels are largely independently regulated during the cell cycle (Figure 1B). Further supporting this conclusion, we did not observe a significant correlation (positive or negative) between exon PSI values and mRNA expression levels for genes with both periodic expression and periodic exon skipping (data not shown). A gene ontology (GO) analysis reveals that genes with periodic AS, like those with periodic transcript level changes (Bar-Joseph et al., 2008; Whitfield et al., 2002), are significantly enriched in cell cycle-related functional categories, including M-phase, nuclear division and DNA metabolic process (Figure 1C; adjusted P <0.05 for all listed categories, FDR <10%) (Supplementary Table1). Similar GO enrichment results were observed when removing the relatively small fraction (10%) of periodically spliced genes that also display significant mRNA expression changes across the cell cycle (Figure 1C). These results thus reveal that numerous genes not previously linked to the cell cycle, as well as previously defined cell cycle-associated genes thought to be constantly expressed across the cell cycle, are in fact subject to periodic regulation at the level of AS (Supplementary File 1 for a full list).

Among the different classes of AS analyzed (cassette exons, alternative 5′/3′ splice sites and intron retention [IR]), periodically regulated IR events were over-represented (relative to the background frequency of annotated IR events) by ~2.2 fold whereas periodically regulated cassette exons, represent the next most frequent periodic class of AS ($P = 2.2\times10^{-16}$, Fisher's exact test, Figure 1-figure supplement 1E). Quantitative RT-PCR assays across different cell cycle stages validated periodic IR events detected by RNA-Seq (Figure 1D). Interestingly, one of these IR events is in transcripts encoding aurora kinase B (AURKB), a critical mitotic factor regulated at the levels of transcription, protein localization, phosphorylation and ubiquitination

(Carmena et al., 2012; Lens et al., 2010). The AURKB retained intron is predicted to introduce a premature termination codon that elicits mRNA degradation through nonsense mediated decay, and is thus expected to result in reduced levels of AURKB protein. The splicing of the retained intron lags behind changes in the total *AURKB* mRNA expression (Figure 1E). We computationally corrected levels of fully spliced, protein coding *AURKB* mRNA by taking into account the fraction of intron-retaining (i.e. non-productive) transcripts across the cell cycle stages (Figure 1E). The expression curve for corrected *AURKB* mRNA levels is substantially different from total *AURKB* transcript levels, with a shifted peak coinciding with mitosis. Periodically-regulated IR events detected in other genes, including those with known cell cycle functions such as HMG20B and RAD52, are similarly expected to affect the cell cycle timing of mRNA expression (Figure 1A, 1D). Collectively, these results provide evidence that the temporal control of retained intron AS provides an important mechanism for establishing the timing of expression of AURKB mRNA and protein, as well as of the timing of expression of additional genes during the cell cycle.

The SR protein kinase CLK1 fluctuates during the cell cycle

Alternative splicing is generally regulated by the concerted action of multiple *cis*-elements that recruit cognate splicing factors. Consistently, analysis of our RNA-seq data revealed 96 RNA binding proteins (RBPs) with periodic mRNA expression, including RS domain-containing factors like *SRSF2*, *SRSF8*, *TRA2A* and *SRSF6* (Figure 2-figure supplement 1, 2A, Table 1). These 96 RBPs were significantly enriched in the GO term "splicing regulation" (adjusted $P = 10^{-4}$, Figure 2-figure supplement 2 2B), indicating that periodic AS is likely controlled by multiple RBPs. Correlations between these RBPs and periodic splicing events were

also identified (Figure 2-figure supplement 1, 2C). For example, SRSF2 expression is significantly correlated with the splicing pattern of a retained intron in the *SRSF2* transcript. Further supporting a role for these RBPs in controlling periodic splicing was the identification of RNA motifs bound by a subset of periodically expressed RBPs (Figure 2-figure supplement 1, 2D). To further examine periodic RBP regulation during cell cycle, we measured the abundance of known splicing regulatory proteins at different stages of the cell cycle by immunoblotting (Figure 2A). Among the proteins analyzed, CDC-like kinase 1 (CLK1), an important regulator of the Ser/Arg (SR) repeat family of splicing regulators, displayed the strongest cyclic expression peaking at the G2/M phase (Figure 2A, 2B), consistent with the results of a recent mass-spectrometry-based screen for cycling proteins (Ly et al., 2014). CLK1 is one of four human CLK paralogs (CLK1-4) and is known to regulate AS via altering the phosphorylation status of multiple SR proteins (Duncan et al., 1997; Jiang et al., 2009; Ninomiya et al., 2011; Prasad et al., 1999). Notably, the levels of other detectable CLK paralogs, as well as members of another SR protein kinase, SRPK1, did not change significantly at the level of RNA and/or protein during the cell cycle (Figure 2B and Supplementary File 1).

Given that both CLK1 protein levels and known CLK1 substrates are periodically expressed, we decided to further investigate the role of CLK1 in the context of cell cycle. The levels of total CLK1 mRNA, as well as the levels of specific CLK1 splice variants, did not change significantly during the cell cycle (Figure 2-figure supplement 2, 1A, 1B) indicating that periodic expression of CLK1 is controlled at the level of protein translation and/or turnover. Consistent with this, an exogenously expressed CLK1 protein displayed cell cycle-dependent fluctuations similar to those observed for endogenous CLK1 protein (Figure 2B). Moreover, CLK1 was rapidly degraded upon inhibition of translation by cycloheximide, and this effect was

184 reversed by co-treatment with the proteasome inhibitor MG132 (Figure 2-figure supplement 2
185 1C). Additionally, polyubiquitination of Flag-tagged CLK1 was detected following
186 immunoprecipitation with anti-Flag antibody from cells treated with MG132 (Figure 2–figure
187 supplement 2 1D). These data suggest that the levels of CLK1 protein are controlled by
188 ubiquitin-mediated degradation in a cell cycle-dependent manner.

189 Periodically regulated protein levels are often controlled through negative feedback
190 circuits involving auto-regulatory loops. CLK1 has been reported to auto-phosphorylate on
191 several residues (Ben-David et al., 1991). To investigate whether auto-phosphorylation of CLK1
192 affects its periodic regulation, we tested whether blocking its kinase activity affects its stability.
193 Inhibition of CLK1 kinase activity using a selective inhibitor, TG003 (Muraki et al., 2004),
194 markedly stabilizes both endogenous and exogenously expressed CLK1 proteins (Figure 2C).
195 Moreover, activity-dependent destabilization of CLK1 was observed with a wild type (WT)
196 protein, but not with a catalytically inactive (KD) mutant (Figure 2C, left panel). We further
197 observe that WT CLK1 is rapidly degraded upon cycloheximide treatment, whereas the KD
198 mutant is more stable (Figure 2–figure supplement 1C). We next tested whether CLK1 activity
199 is sufficient to trigger its own degradation by co-expressing KD CLK1 with increasing amounts
200 of WT CLK1. As expected, increasing amounts of WT CLK1 reduces levels of KD CLK1
201 (Figure 2D). Consistent with these results, WT CLK1 is more highly polyubiquitinated compared
202 to the KD mutant (Figure 2E, compare lanes 2 to 4), and treatment with TG003 reduces
203 polyubiquitination levels (Figure 2E, lane 2 *vs.* 3 and lane 4 *vs.* 5). Decreased polyubiquitination
204 of WT CLK1 is more prevalent than is apparent upon TG003 treatment, as CLK1 is stabilized by
205 TG003 inhibition and thus more total Flag-CLK1 is immunoprecipitated (Figure 2E). To further
206 examine whether this auto-feedback loop is required for changes in CLK1 protein levels during

the cell cycle, we treated synchronized cells with TG003 (or DMSO as a control) and measured CLK1 protein levels. We observed that CLK1 inhibition prevents its turnover after the G2/M phase for both endogenous and exogenously expressed kinases (Figure 2F and Figure 2–figure supplement 1E). Taken together, these results provide strong evidence that CLK1 protein levels are controlled by ubiquitin-mediated proteolysis in a cell cycle stage-specific manner, and that an activity-dependent negative feedback loop is required for this periodic regulation. These results further suggest that changes in the levels of CLK1 could account for many of the periodically regulated AS transitions we have detected during the cell cycle.

CLK1 regulates AS events in genes with critical roles in cell cycle control

RNA-Seq analysis of cells treated with TG003 revealed 892 AS events (in 665 genes) that significantly change after CLK1 inhibition (Figure 3A), including known CLK1-regulated splicing events (e.g. exon 4 of CLK1 (Duncan et al., 1997)). It is worth noting that TG003 can also inhibit CLK4 (although to a lesser extent than inhibition of CLK1). However, RNAi of CLK1 is sufficient to recapitulate the phenotype of CLK1/4 inhibition (see below and Figure 4) (Fedorov et al., 2011; Muraki et al., 2004). Intron retention and cassette exons are the most overrepresented types of AS affected by TG003 (Figure 3A). Most (70%) of the CLK1-regulated exons display increased skipping upon CLK1 inhibition, whereas 87% of CLK1-regulated introns show increased retention (Figure 3-figure supplement 1B and 1C), consistent with a recently reported role for CLK1 in the regulation of retained introns (Boutz et al., 2015). Of nine analyzed TG003-affected AS events detected by RNA-Seq analysis, all were validated by semi-quantitative RT-PCR assays (Figure 3B). These observations indicate that CLK1 inhibition mainly suppresses splicing, consistent with a general requirement for phosphorylation of SR

proteins to promote splicing activity (Irimia et al., 2014; Prasad et al., 1999; Tsai et al., 2015). Importantly, there is a significant overlap between genes with cell cycle periodic AS events (Figure 1) and those with CLK1-regulated AS events, involving 156 genes ($P = 8.5\times10^{-10}$, hyper-geometric test). In contrast, consistent with the results in Figure 1, we do not observe a significant overlap between genes containing CLK1-regulated AS events and periodically expressed genes. These results thus support a widespread and rapidly acting role for CLK1 in controlling cell cycle-regulated AS. Indeed, CLK1 inhibition induces rapid (within 3-6 hours) changes in AS among several analyzed cases (Figure 3-figure supplement 1D).

Supporting an important role for CLK1 in cell cycle progression, genes whose AS levels are affected by CLK1 inhibition are significantly enriched in the GO terms cell cycle phase, M-phase, DNA metabolic processes, nuclear division, DNA damage response, and cytokinesis (adjusted $P < 0.05$ and FDR <20% for all listed GO terms; full list in Supplementary File 2). The affected genes function at various stages of cell cycle including the G1/S transition (Figure 3C). Mitotic processes were, however, associated with the largest number of CLK1-target genes with AS changes and included examples that function in centriole duplication (*CEP70, CEP120, CEP290, CEP68, CDK5RAP2*), metaphase and anaphase (e.g. *CENPK, CENPE, CENPN*), and cytokinesis (e.g. *SEPT2, SEPT10, ANLN*) (additional examples in Figure 3C).

To further investigate the functional consequence of CLK1-dependent AS, we selected two examples in genes that have important roles in the cell cycle: *checkpoint kinase 2* (*CHEK2)*, a tumor suppressor that controls the cellular response to DNA damage and cell cycle entry (Paronetto et al., 2011; Staalesen et al., 2004), and *centromere-associated protein E (CENPE)*, a kinetochore-associated motor protein that functions in chromosome alignment and segregation during mitosis (Kim et al., 2008). We detected a TG003 dose-dependent increase in *CHEK2*

exon 9 inclusion, whereas overexpression of WT CLK1 induced exon 9 skipping, an event that removes the CHEK2 kinase domain (Figure 3D). Expression of WT CLK1 in the presence of TG003, or a catalytically inactive CLK1, had little to no effect on the splicing of this exon (Figure 3D, bottom panels), indicating that the catalytic activity of CLK1 is essential for regulating CHEK2 AS. Over-expression of the SR protein splicing regulator SRSF1, a known target of CLK1 (Prasad et al., 1999), had a similar effect as over-expression of CLK1, resulting in CHEK2 exon 9 skipping, whereas knockdown of SRSF1 had the opposite effect (Figure 3D, right panel). Furthermore, the activation of CHEK2 requires homodimerization (Shen et al., 2004), and we observe that the CHEK2 isoform lacking exon 9 still interacts with full-length protein (Figure 3-figure supplement 1E), suggesting that this CLK1-regulated isoform may function in a dominant-negative manner to attenuate CHEK2 activity.

CENPE is known to be tightly controlled at multiple levels (including transcription, localization, phosphorylation and degradation), and disruption of its regulation leads to pronounced mitotic defects. *CENPE* AS generates long and short isoforms (Supplementary File 2), with the predominant variant being the short isoform that lacks amino acids 1972-2068. Inhibition of CLK1 rapidly shifts *CENPE* splicing to produce predominantly the long isoform (Figure 3E), and this is accompanied by a reduction in *CENPE* protein levels during G2/M phase, presumably due to the instability of the long isoform (Figure 3E). These data thus show that CLK1 controls the AS of major cell cycle regulators, and therefore suggest that inhibition of CLK1 may alter cell cycle progression.

To investigate this, we next performed an RNA-Seq analysis of synchronized cells at G1 and early G2 (when CLK1 accumulates), following inhibition of CLK1 with TG003. As a specificity control, we performed a parallel RNA-Seq analysis using a structurally distinct CLK1

inhibitor, KHCB-19 (Fedorov et al., 2011). Strikingly, of 1,498 AS events that change between G1 (*t=0*) and G2 (*t=6*) ~94% display reduced changes following treatment with the two drugs (Figure 3F), with 65% commonly affected by both drugs, thus supporting an important role for CLK1 in controlling cell-cycle dependent splicing.

CLK1 is Required for Normal Mitosis and Cell Proliferation

Given that CLK1 regulates the AS of many cell cycle factors (Figure 3C), we next examined whether it is necessary for cell cycle progression. Knockdown of CLK1 using shRNAs led to an accumulation of cells with 4N DNA content in multiple cell types, specifically HeLa, H157, and A549 (Figure 4A, Figure 4-figure supplement 1 1A, 1B), and the extent of this accumulation correlated with the degree of knockdown (Figure 4-figure supplement 1 1A). We also observed a significant increase in multi-nucleation, a common consequence of defective chromosome segregation or cytokinesis, following shRNA-knockdown or TG003 inhibition of CLK1 in the treated cells (Figure 4B and Figure 4-figure supplement 1 1C). To visualize the effect of CLK1 inhibition on mitosis at a single cell level, we performed time-lapse high-content microscopy on live cells stably expressing a GFP-histone 2B fusion protein, to track changes in chromatin. TG003-treated cells entered mitosis normally, as measured by nuclear envelope breakdown, but displayed delayed or aberrant cytokinesis, typically resulting in multi-polar divisions, increased time in metaphase, failure to undergo chromatin de-condensation and eventual cell death (Figure 4C and Video 1-5). To further determine at what cell cycle stage CLK1 activity is required, we inhibited CLK1 using TG003 at different time points after early S phase release. Consistent with the imaging data, both control and TG003-treated cells entered mitosis normally, as measured by 4N DNA content. However, inhibition of CLK1 before late S-

phase impaired progression through mitosis, whereas cells treated 5 hours after early S phase release underwent a round of normal mitotic division, although failed to enter the next cell cycle (Figure 4D and Figure 4-figure supplement 1 1D). These results suggest that the primary defects caused by CLK1 inhibition occur in late S-phase and G2 phase, which is when CLK1 levels normally begin to rise (Figure 2A). This conclusion is further supported by the observation that CLK1-dependent AS targets, such as those detected in *HMMR* and *CENPE,* are periodically expressed during cell cycle and peak during G2 and M phase (Figure 4-figure supplement 1 1E). Taken together with the earlier results, these data support an important and multifaceted role for CLK1 in the control of cell cycle progression through its function in the global regulation of periodic AS.

CLK1 expression and CLK1-regulated AS is altered in kidney cancer

The importance of CLK1 for faithful progression through the cell cycle suggests it may play a role the control of cell proliferation in cancer. Supporting this, shRNA knockdown or chemical inhibition of CLK1 with TG003 or KHCB-19 in HeLa cells results in a near complete block in cell proliferation, as measured by anchorage-dependent and -independent colony formation assays (Figure 4E and Figure 4-figure supplement 1F). As mentioned above, CLK1 is likely the primary target of inhibition in these experiments since RNAi of CLK1 recapitulates the phenotype seen with these chemical inhibitors.

Using RNA-Seq data from the Cancer Genome Atlas (TCGA) (Cancer Genome Atlas Network, 2013) we observe that CLK1 displays significantly higher expression in 72 kidney tumors compared to matched normal tissue samples (Figure 4F, $P = 10^{-5}$, Kolmogorov-Smirnov test). Consistently, most CLK1-controlled AS events that are altered in tumors have expected

splicing changes (Figure 4-figure supplement 2 2A). Furthermore, patients with tumors that have elevated CLK1 expression (i.e. the upper quartile of all samples) have significantly lower survival rates relative to other patients in the comparison group (Figure 4G, $P = 0.007$). While there was also an increase in CLK2, CLK3 and CLK4 mRNA expression in these tumors, CLK1 displayed the highest relative mRNA expression levels compared to CLK2 and CLK3 (Figure 4-figure supplement 2 2B). Levels of the CLK4, which is ~80% identical to CLK1, did not correlate with survival differences despite its increased levels in tumors (Figure 4-figure supplement 2 2C). Consistent with this, CLK1-regulated AS events, as defined by the RNA-Seq analysis in Figure 3, were also altered across multiple tumor types, including breast, colon, lung and liver (Figure 4H and Figure 4-figure supplement 2 2D). These data are further consistent with a multi-faceted role for CLK1 in regulating cell cycle progression, and also suggest that CLK1 contributes to increased cell proliferation in cancer, at least in part through its role in controlling periodic AS.

Discussion

Previous studies have shown that splicing and the cell cycle are intimately connected processes. Indeed, cell cycle division (CDC) loci originally defined in *S. cerevisiae,* namely *cdc5* and *cdc40*, were subsequently shown to encode spliceosomal components (Ben-Yehuda et al., 2000; McDonald et al., 1999). Moreover, genome-wide RNAi screens for new AS regulators of apoptosis genes in human cells revealed that factors involved in cell-cycle control, in addition to RNA processing components, were among the most significantly enriched hits (Moore et al., 2010; Tejedor et al., 2015). An RNAi screen performed in *Drosophila* cells for genes required for cell-cycle progression identified numerous splicing components(Bjorklund et al., 2006) as

345 well as a *Drosophila* ortholog of CLK kinases, *Darkener of apricot Doa* (Bettencourt-Dias et al.,
346 2004). In other studies, negative control of splicing during M phase was shown to be dependent
347 on dephosphorylation of the SR family protein, SRSF10 (Shin and Manley, 2002), and the
348 mitotic regulator aurora kinase A (AURKA) was shown to control the AS regulatory activity of
349 SRSF1(Moore et al., 2010). Our study shows for the first time that AS patterns are subject to
350 extensive periodic regulation, in part via a global control mechanism involving cell cycle
351 fluctuations of the SR protein kinase CLK1. At least one likely function of this periodic AS
352 regulation is to control the timing of activation of AURKB (Figure 1), as well as of numerous
353 other key cell cycle factors shown here to be subject to periodic AS. The definition of an
354 extensive, periodically-regulated AS program in the present study thus opens the door to
355 understanding the functions of an additional layer of regulation associated with cell cycle control
356 and cancer.

357 Since many RBPs are found to be periodically expressed (Fig. 4A), it is likely that other
358 aspects of mRNA metabolism are also coordinated with cell cycle stages. For example,
359 differential degradation could potentially contribute to the observed periodic fluctuation of splice
360 isoforms during cell cycle. The degradation of mRNA is closely linked with alternative
361 polyadenylation, which has emerged as a critical mechanism that controls mRNA translation and
362 stability. Generally, shortened 3′ UTRs are found in rapidly dividing cells and more aggressive
363 cancers (Mayr and Bartel, 2009). This study identified 94 cases periodic alternative poly-A site
364 usage (data not shown) in genes known to regulate cell cycle and/or proliferation, including
365 *SON*, *CENPF and EPCAM* (Ahn et al., 2011; Bomont et al., 2005; Chaves-Perez et al., 2013). In
366 addition, many mRNAs have recently been found to be translated in a cell cycle dependent
367 fashion (Aviner et al., 2015; Maslon et al., 2014; Stumpf et al., 2013). Interestingly, a fraction of

368 periodically translated genes are also periodically spliced, including key regulators of cell cycle
369 (e.g., *AURKA*, *AURKB*, *TTBK1* and *DICER1*). This observation is consistent with recent findings
370 that the regulation of AS and translation may be coupled (Sterne-Weiler et al., 2013). In
371 summary, we have demonstrated that AS is subject to extensive temporal regulation during the
372 cell cycle in a manner that appears to be highly integrated with orthogonal layers of cell cycle
373 control. These results thus provide a new perspective on cell cycle regulation that should be
374 taken into consideration when studying this fundamental biological process, both in the context
375 of normal physiology and diseases including cancers.
376

Methods

Cell culture and synchronizations: HeLa (a kind gift from J. Trejo), HEK 293T (from ATCC CRL-3216) and A549 (kind gift from W. Kim) cells were maintained in DMEM (Gibco) medium supplemented with 10% FBS (Gibco). All cells were cultured in humidified incubators with 5% CO_2. Cell cycle synchronization was adapted from the protocol of Whitfield et al. (Whitfield et al., 2002); ~ 750,000 log phase HeLa cells were plated in 15 cm dishes in complete media and allowed to attach for 16 hrs, reaching < 30% confluence. Cells were subsequently treated with 2 mM thymidine (Sigma) for a total of 18 hrs, washed 2 times with 1xPBS, and supplemented with fresh complete media for 10 hrs. 2 mM thymidine was subsequently added for a second block of 18 hrs and washed as described previously. Mitotic block was performed by double thymidine arrest (as above) and release in fresh media for 3.5 hrs followed by addition of nocodazole 100 μM (Sigma) for 10 hrs. G1 block was performed by serum starvation for 72 hrs in DMEM containing 0.05% FBS. For RNA-Seq, cells (both adherent and detached) were harvested every 1.5 hrs for 30 hrs and frozen immediately for purification of total RNA. To block the activity of CLK1, cells were treated with TG003 (Sigma), KHCB-19 (Tocris). To block activity of the proteasome cells were treated with MG132 (Sigma). Drugs were-suspended in DMSO and added to growing cultures at the indicated concentrations and times.

Flow cytometry and cell cycle analysis: Cells were harvested with trypsin treatment, washed 2 times in cold 1xPBS and subsequently fixed in 80% ice cold ethanol for at least 4 hrs. Cells were then washed twice with 1xPBS and suspended in propidium iodide/RNase staining buffer (BD Pharmingen, cat # 550825). Cells were analyzed by flow cytometry to count 10,000 cells that satisfied gating criteria. Data collected were analyzed using ModFit software to discern 2N (G1), S-phase, and 4N (G2 and M) composition.

Mapping and filtering of RNA-Seq data: RNA-Seq reads were mapped to the human genome (build hg19) using the MapSplice informatics tool with default parameters (Wang et al., 2010). The mapped reads were further analyzed with Cufflinks to calculate the level of gene expression with FPKM (Fragments Per Kilobase per Million mapped reads) (Trapnell et al., 2010). The levels of alternatively spliced isoforms were quantified with MISO (Mixture-of-Isoforms) probabilistic framework (Katz et al., 2010) using the annotated AS events for human hg19version 2. The levels of alternatively spliced isoforms were also quantified with VAST-TOOLS using the event annotation as previously described (Irimia et al., 2014). Each AS event was assigned a PSI or PIR value to represent the percent of transcripts with the exon spliced in, or the intron retained, respectively.

Identification of periodic AS:

For identification of periodic AS raw PSI/PIR values were normalized as:

$$normalized\ (\Phi_n^s) = \frac{\Phi_n^s - \Phi_{min}^s}{\Phi_{max}^s}$$

where s = 1 to 32,109 for all splicing events; n = 1 to 14 for the 14 samples; Φ_{min} is the minimum and Φ_{max} is the maximum PSI value among the 14 samples.

To identify periodic AS events, normalized gene expression values (normalized FPKM values as e_n) for the well- known periodic gene, *CCNB1*, *CCNA2*, *CCNB2*, and *CENPE*, were used as a starting point to subsequently add curves with broader or sharper peaks as well as shifted to left or right, resulting in 7 periodic expression curves that cover all the phases of cell cycle (Figure 1-figure supplement 1A). We term these "ideal seed curves", which capture intermittent peak times and phase shifts that were not well represented within the initial known

periodic genes. To identify genes with similar splicing patterns across the cell cycle, we computed the Euclidean Distance ED of each AS event s to the model seed curves m as follows:

$$ED_{m,s} = \sum_{n=1}^{14} |normalized\ (e_n^m) - normalized\ (\Phi_n^s)|$$

where m = 1 to 7 for all model seed curves, s = 1 to 32,109 for all AS events.

Based on the ranking of distance, a similar cutoff of $ED \leq 2.75$ was set as a minimum requirement for periodic AS. Lastly, we calculated a false discovery rate (FDR) by shuffling PSI values across the 14 time points 10,000 times and calculating how often a random shuffle had a better periodic score than the true periodic score for that event. A maximum FDR of 2.5% was required for a splicing event to be periodic.

Heat maps, correlations, GO-term analysis, overlap analysis and statistics: Heat maps, hierarchical clustering, and Pearson correlations were generated using GENE-E (www.broadinstitute.org/cancer/software/GENE-E/). All heat maps shown are row-normalized for presentation purposes. Spearman's rank correlation with average linkage was used for clustering. DAVID (http://david.abcc.ncifcrf.gov/gene2gene.jsp) was used for all gene ontology enrichment; terms shown are for biological process (GOTERM_BP_FAT). To test for significance in overlap analysis, overlapping genes in two data sets (i.e. TG003-treatment and periodic AS) and a background set of only co-detected events was used (i.e. genes detected in both experiments). Significance of overlapping gene sets was assessed using the hyper-geometric test. For overlap and correlation analysis between VAST-TOOLS and MISO we used two MISO AS event annotations (HG18 and HG19), due to differences in the input annotation files for these two pipelines. To identify the 4,343 overlapping exons in the heatmap, we used MISO hg19v1

annotations and MISO hg18 annotations, and the VAST-TOOLS annotations. Student's t-test was used to measure significant in cell cycle defects (multi-nucleation and flow-cytometry) as well as semi-quantitative RT-PCR assessment of splice variants. To identify AS events blocked by TG003 or KHCB19, a Student's t-test statistic was used. If a change between G1/S (t=0) and G2 (t=6) was significant, but not significant in the presence of inhibitors we consider that event to be blocked. For over-representation of periodic introns, we performed Fisher's exact test in a 2x2 contingency table as compared to skipped exons. For differences in expression of CLK1 mRNAs in kidney cancers a Kolmogorov-Smirnov test was performed. For survival differences, the *survdiff* function in the R survival package was used (as discussed in methods below).

Plasmid construction, transfections and RNAi: The expression constructs were generated by cloning the cDNA of CLK1 into pCDNA3 (for transient expression) or pCDH (for stable transfection) backbones with different epitope tags (HA or Flag) at the N- or C-terminus. The Myc-His-Ubiquitin expression vector is a gift from Dr. Gary Johnson's lab, and the Histone H2B-GFP expression vector is gift from Dr. Angelique Whitehurst's lab. Plasmid transfections were performed using Lipofectamine 2000 (Invitrogen) according to the manufacturer's protocol. The lentiviral vectors of shRNAs were obtained from Addgene in pLKO.1 TRC cloning plasmid through UNC core facility as part of mammalian gene knockdown consortium. Lentiviral infections were performed according to the manufacturer's instruction from System Biosciences (SBI).

Semi-quantitative RT-PCR assays for monitoring splicing: Cells transfected with shRNA constructs or treated with TG003 were lysed and total RNA was extracted using the Trizol method (Life Technologies). Purified RNA was treated with 1U of RNAse-free DNAase (Promega) for 1 h at 37ºC and reverse transcribed using random hexamer cDNA preparation kit

(Applied Biosystem). One-tenth of the RT product was used as the template for PCR amplification (25 cycles of amplification, with a trace amount of Cy5-dCTP in addition to non-fluorescent dNTPs) using gene specific primers listed in Supplementary File 4. The resulting gels were scanned with a Typhoon 8600 Imager (GE Healthcare), and analyzed with ImageQuant 5.2 software (Molecular Dynamics/GE Healthcare). Real time PCR was carried out using the SYBR Green kit (Invitrogen) and GAPDH as an internal control.

Immunoblotting and immunoprecipitation: Proteins were extracted in lysis buffer (CHAPS 1% w/v, 150 mM NaCl, 50 mM $MgCl_2$ with protease inhibitor), resolved by SDS-PAGE and transferred onto PVDF membrane. For immunoprecipitaion experiments to detect ubiquitination, cells were co-transfected with Flag-CLK1 and myc-ubiquitin constructs as above. 36 hrs later, TG003 (20 μM) was added for 18 hrs. 4 hours prior to harvesting, 10 μM of MG132 was added to the media. Proteins were extracted in lysis buffer as above with the addition of NEM. Incubation with EZ-View FLAG Beads (Sigma) was performed for 2 hrs at 4^{o}C. Samples were extensively washed according to the manufacturer's protocol and subjected to immunoblotting. Antibodies and dilutions are listed in Supplementary File 4.

Immunofluorescence and high-content live-cell imaging: For immunofluorescence microscopy, cells were plated on glass coverslips coated with poly-L-Lysine. Cells were then washed twice with 1xPBS, fixed with 4% formaldehyde (Sigma), permeabilized with 0.05% Triton X-100 (Promega) and blocked with 3% BSA (Fisher); all dilutions were made in 1XPBS. For live cell imaging, HeLa cells transduced with Histone H2B-GFP was stably selected as described previously (Cappell et al., 2010). Cells were plated in a 6-well format and treated with 2 mM thymidine for 24 hrs, subsequently washed and released in fresh complete medium with or

485 without TG003 (20 μM). Cells were imaged using the BD Pathway Microscope with a 10X
486 objective.

487 **Colony formation assays:** HeLa cells stably producing shRNAs targeting CLK1 or control
488 shRNAs were plated at low density (1,000 cells/6 cm^2) in standard culture medium and allowed
489 to proliferate for 9 days. Cells were then fixed and stained with crystal violet at room
490 temperature. The dried plates were used for estimations of colony diameter and number.

491 **Kidney Cancer Analysis of CLK1 and Alternative Splicing:**

492 RNA-Seq data from the The Cancer Genome Atlas (Ciriello et al., 2013) was processed as
493 previously described (Tsai et al., 2015). Briefly, for mRNA expression, RSEM expression values
494 for the indicated genes were analyzed in 79 paired KIRC (tumor and normal) samples and the
495 paired ks-test was used to test significance. For alternative splicing analysis data from BRCA:
496 Breast invasive carcinoma, COAD: Colorectal adenocarcinoma, KIRC: Kidney renal clear cell
497 carcinoma, LUAD: Lung adenocarcinoma, LUSC: Lung squamous cell carcinoma, LIHC: liver
498 hepatocellular carcinoma were analyzed through the MISO pipeline as described above (Tsai et
499 al., 2015). Relapse-free survival was analyzed using Kaplan Meier plots. All plots and statistical
500 analyses (*survdiff*) were generated using the R package version 3.1.1 *survival* function.
501

Acknowledgements:

We thank Dr. Jan Prins and Darshan Singh for helpful suggestions in analyzing RNA-Seq data, and Drs. Angelique Whitehurst, William Marzluff and Jean Cook for sharing reagents. We thank Drs. Jun Zhu and Ting Ni for advice and assistance in generating strand-specific RNA library. Dr. Rebecca Sinnott provided assistance in live cell imaging experiments. We thank Drs. William Marzluff, Chris Burge, Jean Cook, Michael Emanuele and Mauro Calabrese for helpful comments on the manuscript. This work is supported by an NIH grant (R01CA158283) and Jefferson-Pilot fellowship to Z.W., and by grants from the Canadian Institutes of Health Research to B.J.B. B.J.B. holds the Banbury Chair of Medical Research at the University of Toronto.

Author Contributions:

D.I.D. and Z.W. conceived the project design, and D.I.D. performed the experiments. Y.-H.T., D.I.D., R.W., Y.W., B.J.B. and Z.W. analyzed data. D.I.D., Z.W. and B.J.B. wrote the paper with input from other authors.

Disclosure of Potential Conflicts of Interest

No potential conflicts of interest to disclose by the authors of this work.

Supplemental Information:

Supplementary File 1. Periodic splicing events identified during the HeLa cell cycle and associated GO terms. Data associated with Figure 1

Supplementary File 2. AS events altered by CLK1 inhibition (TG003 10μM for 16hrs) in 293T cells and associated GO terms. Data associated with Figure 3.

Supplementary File 3. AS events altered by CLK1 inhibition (TG003 10μM, KHCB19 10μM) in synchronized HeLa cells. Data associated with Figure 3.

Supplementary File 4. List of PCR primers, shRNA sequences and antibodies used in this study.

Video 1. Live-cell imaging of control HeLa cells stably expressing a GFP-H2B. Cells were synchronized by single-thymidine block and released and imaged at 10X magnification (every ~15 min) for 960 min.

Video 2. Live-cell imaging of control HeLa cells stably expressing GFP-H2B. Cells were synchronized by single-thymidine block and released into 1 μM of TG003 and imaged at 10X magnification (every ~15 min) for 960 min.

Video 3. Zoom of live-cell imaging of control HeLa cells. Data associated with Figure 4D.

Video 4. Zoom of live-cell imaging of TG003-treated HeLa cells. Data associated with Figure 4

Video 5. Zoom of live-cell imaging of TG003-treated HeLa cells. Data associated with Figure 4

Main Figure Legends

Figure 1: Global detection of periodic cell cycle-dependent alternative splicing.

A, Heat map representation of periodically spliced events. Row-normalized relative PSI values are shown. Diagram below indicates cell cycle phase.

B, Overlap between periodically spliced genes and periodically expressed genes detected by RNA-Seq.

C, Heat map representation of enriched Gene Ontology terms shown as log(*P*-value). Three gene sets were analyzed separately: all genes with periodic AS, genes with periodic AS only, and genes with both periodic AS and periodic expression.

D, Real-time quantitative PCR analysis of periodic retained introns and total mRNAs for three selected genes. Cells were synchronized by double thymidine block and samples were collected 0, 3, 6, 9, 12 and 15 hours post release. Errors bars represent standard deviation of the mean. Diagram below indicates cell cycle stage.

E, Schematic representation of *AURKB* AS pattern. Line graph showing the relationship between intron retention and mRNA levels for the *AURKB* gene across the cell cycle. Percent intron retention (solid red line) across cell cycle was used to determine the fraction of total mRNAs (solid blue line) not containing an intron, i.e. 'corrected' mRNA levels (dashed blue line).

Figure 2: Cell cycle-dependent regulation of CLK1.

A, Immunoblot analysis of proteins involved in splicing regulation in synchronized HeLa cells after release from double thymidine block.

B, Immunoblot analysis of selected proteins in asynchronous HeLa cells or cells arrested at different cell cycle stages. Stably expressed exogenous CLK1 levels were also assessed during the cell cycle (bottom panel).

C, Immunoblot of endogenous CLK1 (top) and exogenously-expressed wild type ($CLK1_{wt}$) or kinase catalytically inactive ($CLK1_{KD}$) proteins (bottom) upon treatment with 10 μM TG003.

D, Co-expression of $CLK1_{WT}$ and $CLK1_{KD}$ at different ratios.

E, Immunoprecipitation of CLK1 proteins co-expressed with myc-ubiquitin. Cells were treated with 10 μM TG003 and 10 μM MG132 prior to sample collection.

F, Immunoblot analysis of lysates from cells synchronized upon early S phase (double thymidine) release with or without TG003 treatment.

Figure 3: CLK1 regulates a network of genes that control cell cycle progression.

A, Identification of endogenous CLK1 targets by RNA-Seq. Numbers of different AS types affected by treatment with the CLK1 inhibitor TG003 (left graph). SE, skipped exon; RI, retained intron; A3E, alternative 3′ exon; A5E, alternative 5′ exon. Fraction of total analyzed events that were affected by TG003 treatment (right graph).

B, Validation of TG003-responsive AS events by semi-quantitative RT-PCR. The bar graph shows the max-delta PSI for each AS event tested in a 24-hour time course of inhibition with 20μM TG003.

C, Representation of cell cycle control genes with CLK1-dependent AS events, organized by cell cycle phase and function.

D, Schematic representation of CHEK2 alternative splicing, showing that exon 9 encodes a region overlapping the kinase domain (upper panel). Semi-quantitative RT-PCR assessment of

CHEK2 isoforms after treatment with TG003 or over-expression of the indicated factors (lower left panel). RNAi of SRSF1 in cells and subsequent analysis of CHEK2 splicing by semi-quantitative RT-PCR (lower right panel). PSI values are shown below gel.

E, Normalized *CENPE* total mRNA expression during an unperturbed cell cycle (triangle denotes mitosis, left panel) and diagram of *CENPE* splicing (right). TG003-treatment of HeLa cells released from G1/S arrest followed by semi-quantitative RT-PCR analysis of CENPE isoforms (bar graph).

F, Schematic of RNA-Seq analysis of CLK1 inhibition during cell cycle (left). AS events that were identified as being differentially regulated between G1 and G2 phase (top bar of bar graph) and number of events that were blocked by the indicated conditions (bottom 4 bars).

Figure 4: **CLK1 is required for cell cycle progression and proliferation.**

A, Immunoblot analysis of CLK1 proteins after stable shRNA knockdown in HeLa cells. Bottom, DNA content as measured by propidium iodide staining following flow cytometry.

B, Immunofluorescence microscopy of A549 cells depleted of CLK1 by shRNA (top row), cells treated with 10 μM TG003 for 12hrs (middle row), and a control treatment with DMSO (bottom row); green: tubulin, red: emerin (nuclear envelope), and blue: DAPI. Scale bar 10 μm. Right bar graph shows the quantification of multinucleated cells. *P* values determined using Student's t-test.

C, Static frames from a live-cell high-content imaging movie of HeLa cells expressing Histone H2B-GFP and treated with TG003 (top panel). Time after start of the experiment is indicated; EP, end point (~960 min). TG003 treated cells with apparent cell division defects (indicated by arrowheads in the bottom field) are shown in two independent fields.

D, Synchronized HeLa cells were treated with 20 μM TG003 at the indicated time points (0, 5, and 10 hrs) and analyzed by propidium iodide staining and flow cytometry to measure DNA content. Percent of 2N (lower bar graph) and 4N (upper bar graph) cells were quantified at each time point as indicated in the treatment scheme (top).

E, Colony formation assay of HeLa cells depleted of CLK1 by shRNA, or continuously treated with TG003 or KHCB-19 at the indicated concentrations.

F, Box plot representation of CLK1 mRNA expression levels in paired normal and tumorous kidney tissue. 72 cases were analyzed.

G, Kaplan-Meier plot showing survival differences between patients with kidney tumors with high CLK1 (red, upper quartile) or reduced CLK1 (blue, lower three quartiles) expression.

H, Number of cancer-associated AS events that are also regulated by CLK1 in different tumor types. BRCA, Breast invasive carcinoma; COAD, Colorectal adenocarcinoma; KIRC, Kidney renal clear cell carcinoma; LUAD, Lung adenocarcinoma; LUSC, Lung squamous cell carcinoma; LIHC, liver hepatocellular carcinoma.

Legends for figure supplements

Figure 1 –figure supplement 1: Identification of periodic AS by multiple analysis pipelines.

A, Number of sequencing reads per sample (top). RNA-Seq reads and periodic seeds used for the identification of all periodically expressed and spliced genes (bottom, see methods).

B,C, Dot plot of periodic score and false discovery rate (FDR) for each exon analyzed by the MISO and VAST-TOOLS analysis pipelines. Dashed lines show FDR and periodic score cutoff (see methods).

D, Heat map representation of periodically-spliced events identified by the VAST-TOOLS pipeline. Data are row-normalized. Diagram below indicates cell cycle stage.

E, Bar graphs showing the number of periodic AS events identified separated by event type and shown as a fraction of total events identified (SE: skipped exon, RI: retained intron, A3: alternative 3'splice site, A5: alternative 5'splice site). MISO analysis (left panel in blue) and VAST-TOOLS analysis (right panel in red).

F, Venn diagram representation of the overlap between periodic AS identified by VAST-TOOLS and periodically expressed mRNAs (top). Venn diagram representation of the overlap between periodic AS events as identified by both VAST-TOOLS and MISO (bottom, see methods).

G, Spearman's rank correlation analysis of each cell cycle time point according to commonly detected alternative exons by MISO and VAST-TOOLS. Spearman's rho values are shown in heat map.

Figure 2 –figure supplement 1: Periodic expression of RBPs

(A) Heat map representation of RNA-bound proteins (RBPs) with periodic expression. Row-normalized FPKM levels are shown.

(B) GO analyses for the functional enrichment in the periodic RBPs.

(C) Number of periodic AS events that significantly correlate (Spearman's Rho > |.75|, $P < .05$) with the expression pattern of each RBP during cell cycle. Expression pattern of known two known splicing factors, SRSF2 and ESRP2, is shown in inset.

(D) Average PSI values of periodic that peak at either G1 (red line) or M phase (blue line) (top panel). k-mer enrichment in periodic exons as judged by Z score and separated by cell cycle phase (y-axis = G1-S and x-axis = G2-M) (bottom panel).

Figure 2 –figure supplement 2: Regulation of CLK1 proteins levels during the cell cycle is degradation-dependent.

A, *CLK1* mRNAs as measured in synchronized cells by RNA-Seq (left) or in cells arrested at each cell cycle phase, followed by quantitative RT-PCR (right).

B, Diagram depicting alternative the splicing pattern for *CLK1* pre-mRNA (left). The short form represents skipping of exon 4 that introduces a premature stop codon and is targeted by the non-sense mediated decay pathway, while long form represents the full-length active isoform. Right panels show levels of CLK1 variants, as measured by semi-quantitative RT-PCR with primers that simultaneously detect both forms, in cells upon early S phase release or in cells arrested at specific stages.

C, Protein stability of CLK1 is affected by its activity. Cyclohexamide chase experiment was used to measure the stability of CLK1 in cells expressing either $CLK1_{wt}$ or the catalytic mutant $CLK1_{KD}$. MG132 was used to block proteasomal degradation.

D, Immunoprecipitation of Flag-CLK1 from cells after 3hrs of MG132 treatment and subsequent detection of polyubiquitination by immonoblotting. The arrow indicates the expected position of unmodified CLK1. Bottom panel shows FLAG-CLK1 protein.

E, HeLa cells stably expressing Flag-CLK1 were synchronized by double thymidine block in the presence or absence of TG003. Phosphorylated histone 3B was detected as cell cycle marker.

Figure 3 –figure supplement 1: CLK1 regulates a network of genes that control cell cycle progression.

A, Identification of endogenous CLK1 targets by RNA-Seq. Cells were treated with 10 μM TG003 for 18hrs and poly-A+ RNA was sequenced. Genes significantly up-regulated or down-regulated upon CLK1 inhibition (log(FPKM) are plotted, all plotted genes meet $P < 10^{-7}$).

B, Scatter plot representation of cassette exon inclusion after TG003 treatment by MISO analysis. Log Bayes factor values are shown on y-axis and delta PSI on x-axis.

C, Scatter plot representation of retained intron levels after TG003 treatment. Log Bayes factor values are shown on y-axis and delta PSI on x-axis.

C, Time course experiment after TG003 treatment. Cells were collected at the indicated time points and the absolute delta PSI is plotted.

E, Immonoblot analysis of reciprocal co-immunoprecipation experiments between CHEK2 isoforms as indicated.

Figure 4 –figure supplement 1: Loss of CLK1 results in cell cycle defects in multiple cell types.

A, Cell cycle composition as measured by propidium iodide staining of DNA and flow cytometry analysis of cells that have been depleted of CLK1 by the indicated shRNAs.

B, Representative histograms of propidium iodide stained H157cells to determine cell cycle defect after RNAi of CLK1.

C, HeLa cells treated with TG003 also have defective cell division. Immunofluorescence microscopy was used to detect multi-nucleated cells, and a representative field is shown (green:tubulin, red:emerin, blue:DAPI).

D, Representative histograms of DNA content in synchronous HeLa cells treated with TG003. The time after early S phase release (when TG003 was added) is indicated, These data are associated with Figure 4 of the main text.

E, Representative image from anchorage-independent growth assays (soft agar assay) of HeLa cells after depletion of CLK1.

F, Relative mRNA expression levels of *CENPE* and *HMMR* during cell cycle. Data obtained from RNA-Seq analysis. Dashed line represents 6 hours after release from G1/S.

Figure 4 –figure supplement 2: CLK1 mis-regulation in human cancer

A, Overlap of AS events that were altered in kidney cancers (as compared to normal kidney samples) and AS that was altered in asynchronous cells treated with TG003 (left panel). Pie chart denoting if AS in cancer occurred in the expected direction, that is, normal kidney resembled TG003 treatment while tumor kidney resembled untreated cells (see methods).

B, Boxplot representation of CLK1, CLK2, CLK3 and CLK4 mRNA levels in 72 paired normal vs. cancer kidney cancer (cRCC) samples. Kolmogorov-Smirnov test significance for each factors is as follows CLK1: $P = 3 \times 10^{-5}$, CLK2: $P = 1.2 \times 10^{-7}$, CLK3: $P = 2.8 \times 10^{-12}$, CLK4: $P = 2.2 \times 10^{-16}$

C, Kaplan-Meier plot of kidney (cRCC) patients with tumors expressing high CLK4 (red, upper quartile) vs. normal CLK4 (blue, 1-3 quartile).

D, PARD3 exon (chr10:34661426-34661464) PSI levels in five cancer cases are shown as an example of TG003-sensitive AS which is altered between normal and cancer tissues.

Reference:

Ahn, E.Y., DeKelver, R.C., Lo, M.C., Nguyen, T.A., Matsuura, S., Boyapati, A., Pandit, S., Fu, X.D., and Zhang, D.E. (2011). SON controls cell-cycle progression by coordinated regulation of RNA splicing. Mol Cell *42*, 185-198.

Aviner, R., Shenoy, A., Elroy-Stein, O., and Geiger, T. (2015). Uncovering Hidden Layers of Cell Cycle Regulation through Integrative Multi-omic Analysis. PLoS Genet *11*, e1005554.

Bar-Joseph, Z., Siegfried, Z., Brandeis, M., Brors, B., Lu, Y., Eils, R., Dynlacht, B.D., and Simon, I. (2008). Genome-wide transcriptional analysis of the human cell cycle identifies genes differentially regulated in normal and cancer cells. Proc Natl Acad Sci U S A *105*, 955-960.

Ben-David, Y., Letwin, K., Tannock, L., Bernstein, A., and Pawson, T. (1991). A mammalian protein kinase with potential for serine/threonine and tyrosine phosphorylation is related to cell cycle regulators. Embo J *10*, 317-325.

Ben-Yehuda, S., Dix, I., Russell, C.S., McGarvey, M., Beggs, J.D., and Kupiec, M. (2000). Genetic and physical interactions between factors involved in both cell cycle progression and pre-mRNA splicing in Saccharomyces cerevisiae. Genetics *156*, 1503-1517.

Bertoli, C., Skotheim, J.M., and de Bruin, R.A. (2013). Control of cell cycle transcription during G1 and S phases. Nat Rev Mol Cell Biol *14*, 518-528.

Bettencourt-Dias, M., Giet, R., Sinka, R., Mazumdar, A., Lock, W.G., Balloux, F., Zafiropoulos, P.J., Yamaguchi, S., Winter, S., Carthew, R.W*., et al.* (2004). Genome-wide survey of protein kinases required for cell cycle progression. Nature *432*, 980-987.

Bjorklund, M., Taipale, M., Varjosalo, M., Saharinen, J., Lahdenpera, J., and Taipale, J. (2006). Identification of pathways regulating cell size and cell-cycle progression by RNAi. Nature *439*, 1009-1013.

Bomont, P., Maddox, P., Shah, J.V., Desai, A.B., and Cleveland, D.W. (2005). Unstable microtubule capture at kinetochores depleted of the centromere-associated protein CENP-F. EMBO J *24*, 3927-3939.

Boutz, P.L., Bhutkar, A., and Sharp, P.A. (2015). Detained introns are a novel, widespread class of post-transcriptionally spliced introns. Genes Dev *29*, 63-80.

Cancer Genome Atlas Network, T. (2013). Comprehensive molecular characterization of clear cell renal cell carcinoma. Nature *499*, 43-49.

Cappell, K.M., Larson, B., Sciaky, N., and Whitehurst, A.W. (2010). Symplekin specifies mitotic fidelity by supporting microtubule dynamics. Mol Cell Biol *30*, 5135-5144.

Carmena, M., Wheelock, M., Funabiki, H., and Earnshaw, W.C. (2012). The chromosomal passenger complex (CPC): from easy rider to the godfather of mitosis. Nat Rev Mol Cell Biol *13*, 789-803.

Chaves-Perez, A., Mack, B., Maetzel, D., Kremling, H., Eggert, C., Harreus, U., and Gires, O. (2013). EpCAM regulates cell cycle progression via control of cyclin D1 expression. Oncogene *32*, 641-650.

Ciriello, G., Miller, M.L., Aksoy, B.A., Senbabaoglu, Y., Schultz, N., and Sander, C. (2013). Emerging landscape of oncogenic signatures across human cancers. Nat Genet *45*, 1127-1133.

David, C.J., and Manley, J.L. (2010). Alternative pre-mRNA splicing regulation in cancer: pathways and programs unhinged. Genes Dev *24*, 2343-2364.

Duncan, P.I., Stojdl, D.F., Marius, R.M., and Bell, J.C. (1997). In vivo regulation of alternative pre-mRNA splicing by the Clk1 protein kinase. Mol Cell Biol *17*, 5996-6001.

Edmond, V., Moysan, E., Khochbin, S., Matthias, P., Brambilla, C., Brambilla, E., Gazzeri, S., and Eymin, B. (2011). Acetylation and phosphorylation of SRSF2 control cell fate decision in response to cisplatin. Embo J *30*, 510-523.

Fedorov, O., Huber, K., Eisenreich, A., Filippakopoulos, P., King, O., Bullock, A.N., Szklarczyk, D., Jensen, L.J., Fabbro, D., Trappe, J*., et al.* (2011). Specific CLK inhibitors from a novel chemotype for regulation of alternative splicing. Chem Biol *18*, 67-76.

776 Grabek, K.R., Diniz Behn, C., Barsh, G.S., Hesselberth, J.R., and Martin, S.L. (2015). Enhanced stability and
777 polyadenylation of select mRNAs support rapid thermogenesis in the brown fat of a hibernator. eLife *4*.
778 Gui, J.F., Lane, W.S., and Fu, X.D. (1994). A serine kinase regulates intracellular localization of splicing
779 factors in the cell cycle. Nature *369*, 678-682.
780 Harashima, H., Dissmeyer, N., and Schnittger, A. (2013). Cell cycle control across the eukaryotic
781 kingdom. Trends Cell Biol *23*, 345-356.
782 Irimia, M., Weatheritt, R.J., Ellis, J.D., Parikshak, N.N., Gonatopoulos-Pournatzis, T., Babor, M., Quesnel-
783 Vallieres, M., Tapial, J., Raj, B., O'Hanlon, D.*, et al.* (2014). A highly conserved program of neuronal
784 microexons is misregulated in autistic brains. Cell *159*, 1511-1523.
785 Jiang, K., Patel, N.A., Watson, J.E., Apostolatos, H., Kleiman, E., Hanson, O., Hagiwara, M., and Cooper,
786 D.R. (2009). Akt2 regulation of Cdc2-like kinases (Clk/Sty), serine/arginine-rich (SR) protein
787 phosphorylation, and insulin-induced alternative splicing of PKCbetaII messenger ribonucleic acid.
788 Endocrinology *150*, 2087-2097.
789 Karni, R., de Stanchina, E., Lowe, S.W., Sinha, R., Mu, D., and Krainer, A.R. (2007). The gene encoding the
790 splicing factor SF2/ASF is a proto-oncogene. Nat Struct Mol Biol *14*, 185-193.
791 Katz, Y., Wang, E.T., Airoldi, E.M., and Burge, C.B. (2010). Analysis and design of RNA sequencing
792 experiments for identifying isoform regulation. Nat Methods *7*, 1009-1015.
793 Kim, Y., Heuser, J.E., Waterman, C.M., and Cleveland, D.W. (2008). CENP-E combines a slow, processive
794 motor and a flexible coiled coil to produce an essential motile kinetochore tether. J Cell Biol *181*, 411-
795 419.
796 Lai, M.C., Lin, R.I., and Tarn, W.Y. (2003). Differential effects of hyperphosphorylation on splicing factor
797 SRp55. Biochem J *371*, 937-945.
798 Lens, S.M., Voest, E.E., and Medema, R.H. (2010). Shared and separate functions of polo-like kinases and
799 aurora kinases in cancer. Nat Rev Cancer *10*, 825-841.
800 Leva, V., Giuliano, S., Bardoni, A., Camerini, S., Crescenzi, M., Lisa, A., Biamonti, G., and Montecucco, A.
801 (2012). Phosphorylation of SRSF1 is modulated by replicational stress. Nucleic Acids Res *40*, 1106-1117.
802 Long, J.C., and Caceres, J.F. (2009). The SR protein family of splicing factors: master regulators of gene
803 expression. Biochem J *417*, 15-27.
804 Ly, T., Ahmad, Y., Shlien, A., Soroka, D., Mills, A., Emanuele, M.J., Stratton, M.R., and Lamond, A.I.
805 (2014). A proteomic chronology of gene expression through the cell cycle in human myeloid leukemia
806 cells. Elife *3*, e01630.
807 Maslon, M.M., Heras, S.R., Bellora, N., Eyras, E., and Caceres, J.F. (2014). The translational landscape of
808 the splicing factor SRSF1 and its role in mitosis. eLife, e02028.
809 Matera, A.G., and Wang, Z. (2014). A day in the life of the spliceosome. Nat Rev Mol Cell Biol *15*, 108-
810 121.
811 Mayr, C., and Bartel, D.P. (2009). Widespread shortening of 3'UTRs by alternative cleavage and
812 polyadenylation activates oncogenes in cancer cells. Cell *138*, 673-684.
813 McDonald, W.H., Ohi, R., Smelkova, N., Frendewey, D., and Gould, K.L. (1999). Myb-related fission yeast
814 cdc5p is a component of a 40S snRNP-containing complex and is essential for pre-mRNA splicing. Mol
815 Cell Biol *19*, 5352-5362.
816 Mocciaro, A., and Rape, M. (2012). Emerging regulatory mechanisms in ubiquitin-dependent cell cycle
817 control. J Cell Sci *125*, 255-263.
818 Moore, M.J., Wang, Q., Kennedy, C.J., and Silver, P.A. (2010). An alternative splicing network links cell-
819 cycle control to apoptosis. Cell *142*, 625-636.
820 Muraki, M., Ohkawara, B., Hosoya, T., Onogi, H., Koizumi, J., Koizumi, T., Sumi, K., Yomoda, J., Murray,
821 M.V., Kimura, H.*, et al.* (2004). Manipulation of alternative splicing by a newly developed inhibitor of
822 Clks. J Biol Chem *279*, 24246-24254.

Ninomiya, K., Kataoka, N., and Hagiwara, M. (2011). Stress-responsive maturation of Clk1/4 pre-mRNAs promotes phosphorylation of SR splicing factor. J Cell Biol *195*, 27-40.
Oltean, S., and Bates, D.O. (2014). Hallmarks of alternative splicing in cancer. Oncogene *33*, 5311-5318.
Pan, Q., Shai, O., Lee, L.J., Frey, B.J., and Blencowe, B.J. (2008). Deep surveying of alternative splicing complexity in the human transcriptome by high-throughput sequencing. Nat Genet *40*, 1413-1415.
Pan, Q., Shai, O., Misquitta, C., Zhang, W., Saltzman, A.L., Mohammad, N., Babak, T., Siu, H., Hughes, T.R., Morris, Q.D*., et al.* (2004). Revealing global regulatory features of mammalian alternative splicing using a quantitative microarray platform. Mol Cell *16*, 929-941.
Paronetto, M.P., Minana, B., and Valcarcel, J. (2011). The Ewing sarcoma protein regulates DNA damage-induced alternative splicing. Mol Cell *43*, 353-368.
Prasad, J., Colwill, K., Pawson, T., and Manley, J.L. (1999). The protein kinase Clk/Sty directly modulates SR protein activity: both hyper- and hypophosphorylation inhibit splicing. Mol Cell Biol *19*, 6991-7000.
Satyanarayana, A., and Kaldis, P. (2009). Mammalian cell-cycle regulation: several Cdks, numerous cyclins and diverse compensatory mechanisms. Oncogene *28*, 2925-2939.
Shen, H., Kan, J.L., and Green, M.R. (2004). Arginine-serine-rich domains bound at splicing enhancers contact the branchpoint to promote prespliceosome assembly. Mol Cell *13*, 367-376.
Shin, C., and Manley, J.L. (2002). The SR protein SRp38 represses splicing in M phase cells. Cell *111*, 407-417.
Staalesen, V., Falck, J., Geisler, S., Bartkova, J., Borresen-Dale, A.L., Lukas, J., Lillehaug, J.R., Bartek, J., and Lonning, P.E. (2004). Alternative splicing and mutation status of CHEK2 in stage III breast cancer. Oncogene *23*, 8535-8544.
Sterne-Weiler, T., Martinez-Nunez, R.T., Howard, J.M., Cvitovik, I., Katzman, S., Tariq, M.A., Pourmand, N., and Sanford, J.R. (2013). Frac-seq reveals isoform-specific recruitment to polyribosomes. Genome Res *23*, 1615-1623.
Stumpf, C.R., Moreno, M.V., Olshen, A.B., Taylor, B.S., and Ruggero, D. (2013). The translational landscape of the mammalian cell cycle. Mol Cell *52*, 574-582.
Tejedor, J.R., Papasaikas, P., and Valcarcel, J. (2015). Genome-wide identification of Fas/CD95 alternative splicing regulators reveals links with iron homeostasis. Mol Cell *57*, 23-38.
Trapnell, C., Williams, B.A., Pertea, G., Mortazavi, A., Kwan, G., van Baren, M.J., Salzberg, S.L., Wold, B.J., and Pachter, L. (2010). Transcript assembly and quantification by RNA-Seq reveals unannotated transcripts and isoform switching during cell differentiation. Nat Biotechnol *28*, 511-515.
Tsai, Y.S., Dominguez, D., Gomez, S.M., and Wang, Z. (2015). Transcriptome-wide identification and study of cancer-specific splicing events across multiple tumors. Oncotarget *6*, 6825-6839.
Vermeulen, K., Van Bockstaele, D.R., and Berneman, Z.N. (2003). The cell cycle: a review of regulation, deregulation and therapeutic targets in cancer. Cell Prolif *36*, 131-149.
Wang, E.T., Sandberg, R., Luo, S., Khrebtukova, I., Zhang, L., Mayr, C., Kingsmore, S.F., Schroth, G.P., and Burge, C.B. (2008). Alternative isoform regulation in human tissue transcriptomes. Nature *456*, 470-476.
Wang, G.S., and Cooper, T.A. (2007). Splicing in disease: disruption of the splicing code and the decoding machinery. Nat Rev Genet *8*, 749-761.
Wang, K., Singh, D., Zeng, Z., Coleman, S.J., Huang, Y., Savich, G.L., He, X., Mieczkowski, P., Grimm, S.A., Perou, C.M*., et al.* (2010). MapSplice: accurate mapping of RNA-seq reads for splice junction discovery. Nucleic Acids Res *38*, e178.
Wang, Y., Chen, D., Qian, H., Tsai, Y.S., Shao, S., Liu, Q., Dominguez, D., and Wang, Z. (2014). The splicing factor RBM4 controls apoptosis, proliferation, and migration to suppress tumor progression. Cancer Cell *26*, 374-389.
Wang, Z., and Burge, C.B. (2008). Splicing regulation: from a parts list of regulatory elements to an integrated splicing code. RNA *14*, 802-813.

Whitfield, M.L., Sherlock, G., Saldanha, A.J., Murray, J.I., Ball, C.A., Alexander, K.E., Matese, J.C., Perou, C.M., Hurt, M.M., Brown, P.O*., et al.* (2002). Identification of genes periodically expressed in the human cell cycle and their expression in tumors. Mol Biol Cell *13*, 1977-2000.

Zhou, Z., and Fu, X.D. (2013). Regulation of splicing by SR proteins and SR protein-specific kinases. Chromosoma *122*, 191-207.

Dominguez Figure-1:

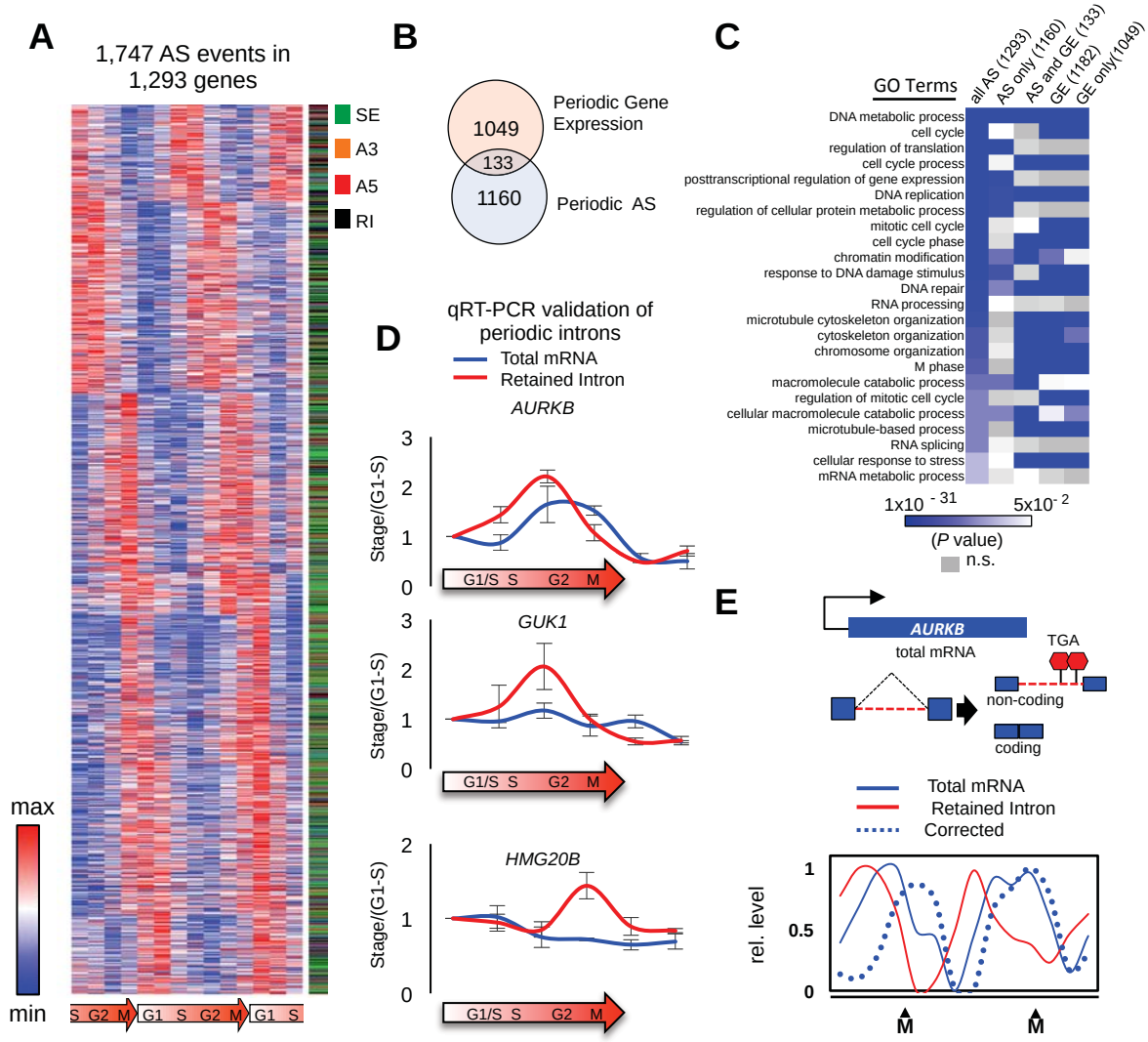

Dominguez Figure-2:

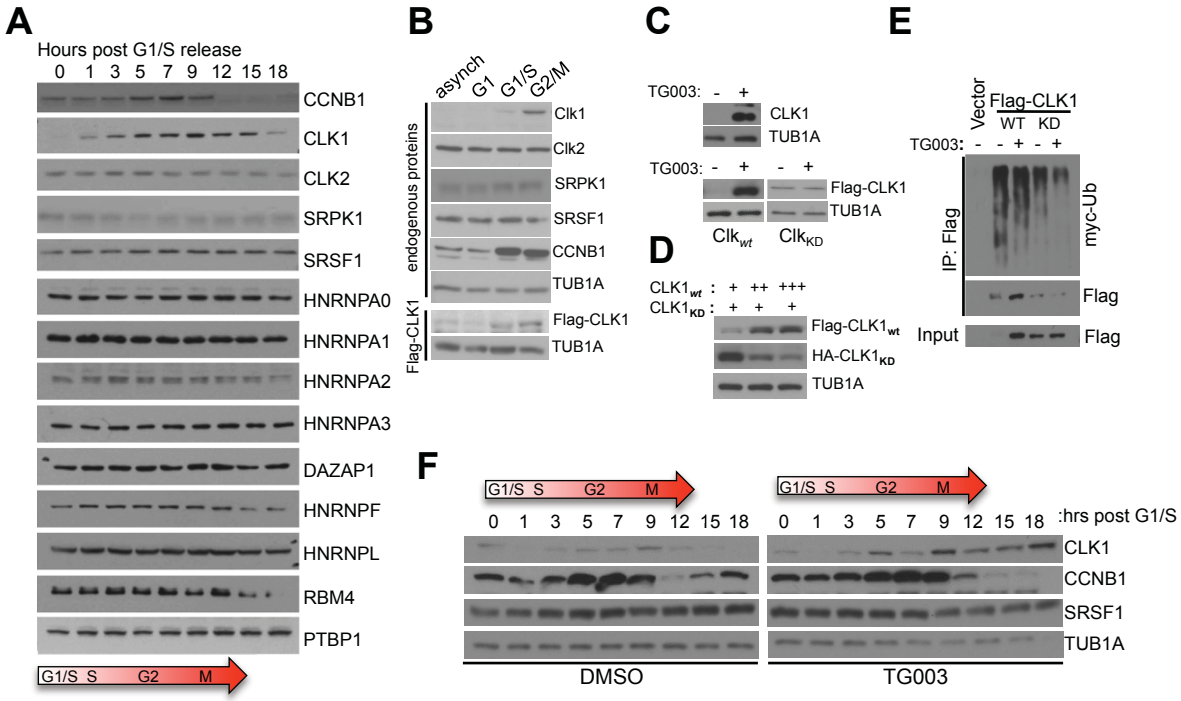

Dominguez Figure-3:

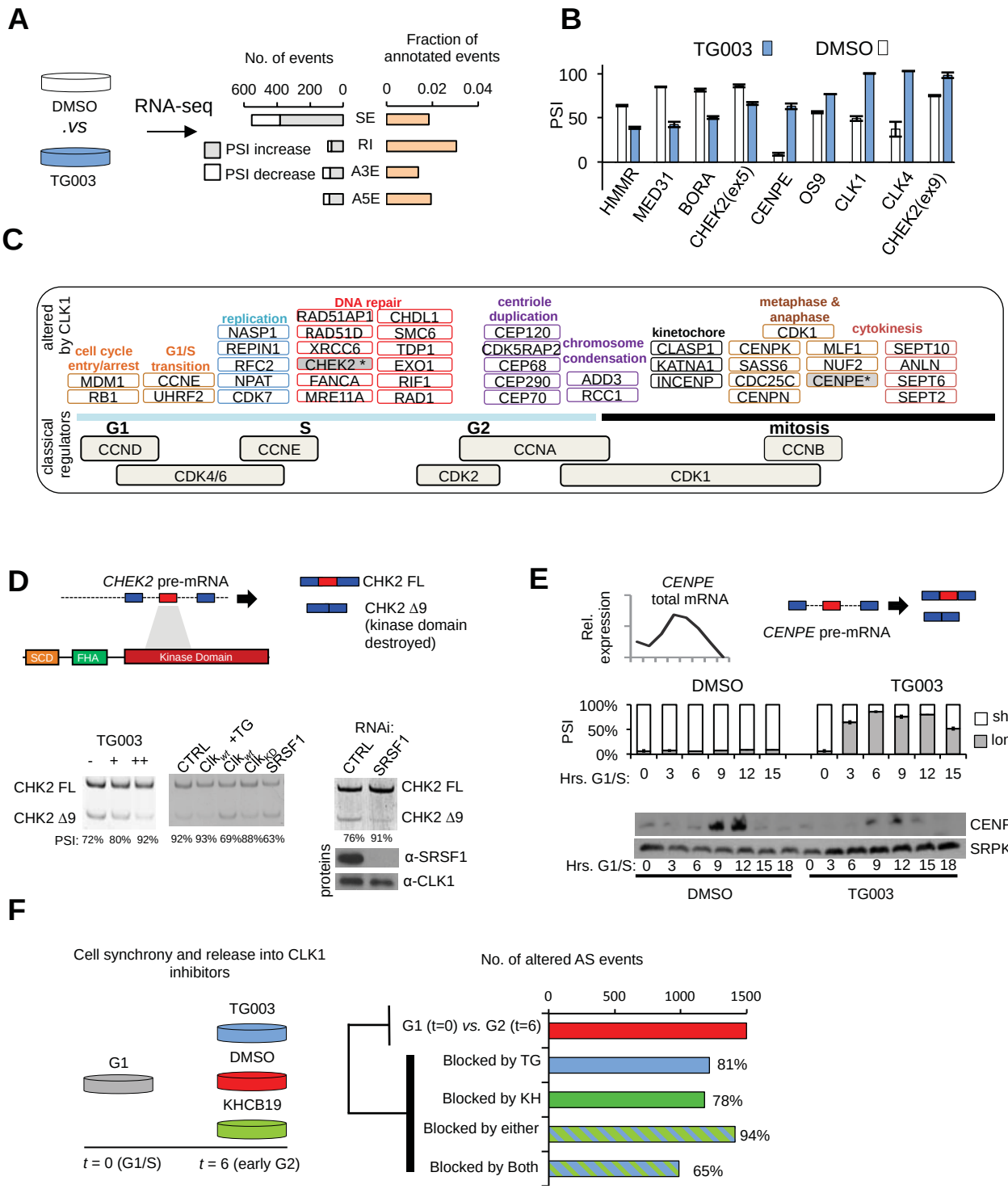

Dominguez Figure-4: